



Time-reversal focusing of ultrashort pulses through thin scattering media

Ohta, Kaoru

(Citation)

Optics Express, 30(4):5486-5497

(Issue Date)

2022-02-14

(Resource Type)

journal article

(Version)

Version of Record

(Rights)

© 2022 Optica Publishing Group. Users may use, reuse, and build upon the article, or use the article for text or data mining, so long as such uses are for non-commercial purposes and appropriate attribution is maintained. All other rights are reserved.

(URL)

<https://hdl.handle.net/20.500.14094/90009571>





Time-reversal focusing of ultrashort pulses through thin scattering media

KAORU OHTA* 

Molecular Photoscience Research Center, Kobe University, 1-1 Rokkodai-cho, Nada, Kobe 657-8501, Japan

*kohta@kobe-u.ac.jp

Abstract: When ultrashort pulses propagate through a disordered medium, scattering occurs and the intensity of the ballistic component decreases drastically. This limits the applicability of time-resolved nonlinear optical spectroscopy and microscopy. The wavefront shaping technique makes it possible to focus light through the scattering medium; however, complete time-reversal of the ultrashort pulses (as short as 10 fs) is still a very challenging problem. This is due to the in-depth characterization and precise control needed for such pulses in the time domain in order to compress down the Fourier-transform limit. In this work, we develop new spatiotemporal wavefront shaping techniques to focus ultrashort pulses at the target position through a thin scattering medium. Compared to other studies, one significant advantage of this method is that most of the characterization of the spectrally-resolved transmission matrix and temporal profile of the ultrashort pulses can be done using single-beam geometry. An interferometer with external reference is necessary to measure the difference of the phase profile between the focused and reference pulses. Furthermore, the number of controllable phase components in the spectral domain is not limited by the spectral correlations of the speckle patterns because we used a pulse shaper in the time domain to optimize the temporal properties of the ultrashort focused pulse. Our new method provides increased flexibility and precise control for manipulating extremely ultrashort pulses through thin scattering media in order to achieve time-reversal focusing at the target position.

© 2022 Optica Publishing Group under the terms of the [Optica Open Access Publishing Agreement](#)

1. Introduction

Ultrashort pulses, as short as tens of femtoseconds, have become routinely available owing to the rapid development of solid-state laser and pulse characterization technologies [1–5]. When using such ultrashort pulses for experiments, dispersion of the optics in the measurement systems must always be characterized and compensated [1–5]. So far, ultrashort pulses are mainly applied in studies of optically homogeneous systems wherein scattering is not so large as to disturb ultrashort pulse propagation. Generally, when coherent light propagates in a scattering medium, the scattered light forms a destructive interference pattern known as “speckle”. This limits the applicability of time-resolved nonlinear optical spectroscopy and microscopy [6–8]. Time-reversal focusing of nearly transform-limited pulse through the scattering media is a very challenging subject because detailed characterization and precise control of both amplitude and phase of the scattered pulse in time domain is very difficult to do in this situation, but quite important to compress and optimize such a pulse. It should be noted that intensity-only measurement of the nonlinear optical signal is not enough to quantify the temporal properties of the ultrashort pulse [5,9]. Recent advances of wavefront shaping techniques have made it possible to focus monochromatic light through scattering media [10–13]. Such techniques have also been applied in broadband light studies, particularly, ultrashort laser pulses [14–20]. Seminal work by Katz *et al.* demonstrated that one can optimize both spatial and temporal distortions of ultrashort pulses through scattering media by only shaping the light in the spatial domain [14]. It was demonstrated that the combination of wavefront shaping in the spatial region with the time-gated reference pulse can be used to optimize the pulse width at the focus spot [15–18]. Gigan *et al.*

developed the multispectral transmission matrix (TM) method to control scattered light both spatially and temporally [19,20].

During the propagation of an ultrashort pulse through multiple scattering media, spread of the photon distribution takes place at the exit of the media. This leads to broadening of the ultrashort laser pulses. Owing to the spatiotemporal coupling of the speckle pattern, one can optimize the pulse width of the output field through the scattering medium using wavefront shaping in the spatial domain. The number of independent phase components in the spectral domain are determined by spectral correlations of the speckle patterns [19,21]. When we consider the contribution of group velocity dispersion in a thin scattering medium, as well as transmission-type optics, wavefront shaping in the spatial domain is insufficient to optimize the temporal property of an ultrashort pulse with a width on the order of 10 fs. This is because the number of independent phase components becomes smaller in a thin scattering medium and the phase of such a pulse depends strongly on the wavelength in a broader spectral region. Furthermore, a few scattering events in thin media are sufficient to significantly distort the temporal profile of the ultrashort pulse, as shown below.

In this work, we develop spatiotemporal wavefront shaping and pulse shaping techniques to control the amplitude and phase of extremely ultrashort pulses through a thin scattering medium. To achieve the best performance for ultrashort pulses, it is important to control spectral phase distortions caused by transmission of the dispersive media. A major advantage of our proposed method is that one can characterize spectrally-resolved TM and temporal profile of ultrashort pulses through scattering media using single-beam geometry in most part of the measurements. For spectral interferometry, we have to use the interferometer with the external reference, but the measurement can be done within a short period of time compared with other ones [22]. As a result, we have high flexibility and reliability in terms of characterization as well as fine control of ultrashort pulses through the scattering medium. We use a paraffin film (Parafilm) as the model system of the thin scattering medium. In the optically thinner media, the scattering mean free path is shorter than the thickness of the sample, but the transport mean free path is longer than the thickness. This means that most of the incident light is scattered, and it propagates in the forward direction, which is the case in biological tissues. Therefore, it is very important to develop the method of the spatiotemporal control of ultrashort pulses in such a situation. By using both wavefront shaping and pulse shaper simultaneously, we can control the spatial and temporal properties of ultrashort pulses through a scattering medium to focus it at the target position in a time-reversed manner.

2. Results

2.1. Spectrally resolved TM measurement of ultrashort pulses

Experimental setup for the spatiotemporal wavefront and pulse shaping technique is shown in Fig. 1(a) and the detail is described in Supplement 1. Figures 1(b) and 1(c) display the spectral and temporal characteristics of the input pulse used for spatiotemporal pulse shaping. The center of the ultrashort pulse spectrum is located at 610 nm, and the bandwidth is about 50 nm. We performed phase measurement and optimization of the ultrashort pulses using the MIIPS (Multiphoton Intrapulse Interference Phase Scan) method [23,24]. In MIIPS measurements, we applied a reference phase function to the phase shaper to cancel the unknown phase profile of the ultrashort pulse. We measured the spectrum of the second-harmonic generation (SHG). When the phase profile of SHG spectrum is expressed by a Taylor expansion and neglect the higher-order terms, SHG spectrum takes a maximum value when the sum of the second-order derivatives of the unknown and reference phase profiles is equal to zero. By iterating the MIIPS measurements, we can obtain the phase profile of the unknown ultrashort pulse in a single-beam geometry [23,24]. The temporal width of the ultrashort pulse was 14 fs. A part of the pulse was used as an external reference pulse only for the spectral interferometry measurement. The optimized

ultrashort pulse propagates through a paraffin film. To characterize the scattering process of the paraffin film, we used a spectrally resolved TM, $T(\lambda)$. In contrast to the previous work, we used the broadband pulse as an input light and the spectrum of the output through the pinhole (diameter of 25 μm) is measured by a spectrometer [19]. This means that the transmitted pulse and the copropagating reference pulse are speckled light fields and the temporal width is stretched by the scattering process and by the dispersion of the transmission-type optics. The external reference pulse was blocked for this measurement, which is different from multispectral or time-gated TM measurements using an external reference light that is closed to transform-limited pulses [15–18].

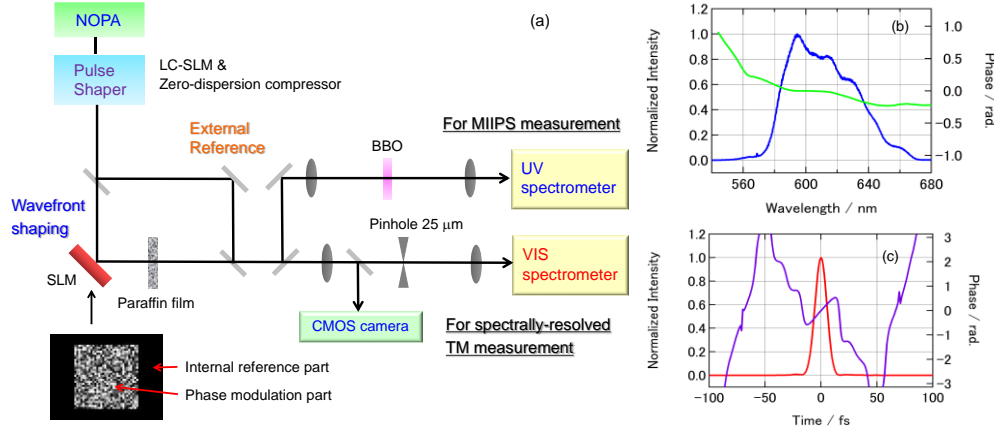


Fig. 1. (a) Schematic diagram of the experimental setup. The ultrashort pulses are split into two after the pulse shaper in the time domain. One pulse is used for wavefront and pulse shaping, and the other is used as an external reference. The SLM display consists of phase modulation and internal reference parts. (b) Spectrum (blue) and phase profile (green) of the ultrashort input pulse after optimization using the MIIPS method. (c) Temporal (red) and phase (purple) profiles of the ultrashort input pulse after optimization of the MIIPS method.

The results of the spectrally resolved TM are shown in Fig. 2. Figure 2(a) shows a phase map of the TM with respect to the wavelength and Hadamard base sets, whereas the Fig. 2(b) shows slices of the TM at three different Hadamard bases. As discussed in the Supplement 1, the spectrally resolved TM is given by the product of the phase modulated field and static reference

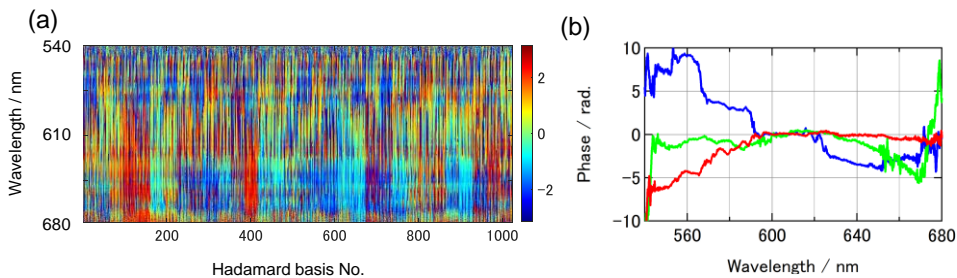


Fig. 2. (a) Phase map of the spectrally resolved TM with respect to the Hadamard base. (b) Phase profile of the spectrally resolved TM at Hadamard basis Nos. 250 (blue), 500 (green), and 750 (red).

field:

$$T_i^{meas}(\lambda) = t_i(\lambda) A^{ref}(\lambda) = |t_i(\lambda)| e^{i(\varphi_i^{TM}(\lambda) - \varphi^{ref}(\lambda))} A^{ref}(\lambda) \quad (1)$$

where i stands for the i -th segment of the SLM, $t_i(\lambda)$ is the i -th element of the TM, and $A_{ref}(\lambda)$ is the amplitude of the copropagating reference field. In Eq. (1), $\varphi_i^{TM}(\lambda_k)$ and $\varphi_{ref}(\lambda_k)$ are the phases of the i -th elements of the TM and static reference fields, respectively. Therefore, the phase profile of the spectrally resolved TM using internal reference speckle fields corresponds to the difference between the phase modulation and the reference parts which is not equal to the phase modulation part itself. To measure this phase difference, we used the four-step phase-shifting method. This means that we change the phase of the reference part of SLM for 0, $\pi/2$, π and $3\pi/2$ to remove the phase-independent terms in Eq. (1) [11].

2.2. Focusing ultrashort pulses at the target position using the spectrally integrated TM

To maximize the transmitted intensity through the pinhole, we calculate the phase conjugation of the spectrally resolved TM and take a summation over a certain wavelength range as follows:

$$S_i^\dagger = \sum_{\lambda_k=\lambda_i}^{\lambda_k=\lambda_f} T_i^{meas}(\lambda_k)^\dagger = \sum_{\lambda_k=\lambda_i}^{\lambda_k=\lambda_f} |t_i(\lambda_k)| e^{-i(\varphi_i^{TM}(\lambda_k) - \varphi^{ref}(\lambda_k))} A^{ref}(\lambda_k) \quad (2)$$

Here, we refer to the matrix in Eq. (2) as the spectrally integrated TM rather than the “broadband” TM. In previous studies of wavefront shaping using broadband TM, a total intensity in the entire wavelength region was measured without resolving each spectral component using a monochromator [25]. In the spectrally integrated TM, summation is made at the wavelength range from λ_i to λ_f . In the current setup, we can only modulate the phase, not the amplitude, in SLM. By applying the phase distribution of Φ_i^+ to the SLM, we can focus the input pulse at a specific target position (see [Supplement 1](#)).

$$\Phi_i = \arg(S_i^\dagger) = \sum_{\lambda_k=\lambda_i}^{\lambda_k=\lambda_f} \{\varphi_i^{TM}(\lambda_k) - \varphi^{ref}(\lambda_k)\} \quad (3)$$

Figure 3 displays the results of an unoptimized speckle pattern and optimized spatially focused spot using phase-conjugated TMs as well as spectra transmitted through the pinhole. In the case of the unoptimized speckle pattern, the size of the speckle depends on the position. At the center of the image, the speckle size is small. Moving from the center to the edge, the speckle size becomes larger. When the scattered pulse is focused by a lens, the overlap of different spectral components depends on the distance from the optical axis at the focal plane, i.e., the overlap becomes smaller from the center to the edge that leads to blurring of the speckle patterns [26]. Details of the contrast change of the speckle patterns are shown in Fig. S4. For the optimized spatially focused spot, the summation of the phase components of TM includes all wavelength regions. The size of the focused spot is determined by the diameter of the pinhole. Measurements and results of speckle correlations with respect to the wavelength are discussed in the [Supplement 1](#) [21]. The spectral width of the correlation is about 4 nm (See Fig. S2). It should be noted that we follow the definition of the spectral correlation width as described in Ref. 20. By analyzing the size of the speckles, we found that the full width at half maximum of the spot size is 17 μm , which is larger than that of the speckles (7–8 μm ; see the [Supplement 1](#)) [10]. This leads to a smaller enhancement factor of the peak intensity versus the background.

Figure 4 displays the spectra of the transmitted pulses through the pinhole before and after taking the phase conjugation of the TM and displaying it to the SLM. As shown in Fig. 4, the spectral shape of the output pulse and enhancement factor depends on the predefined wavelength

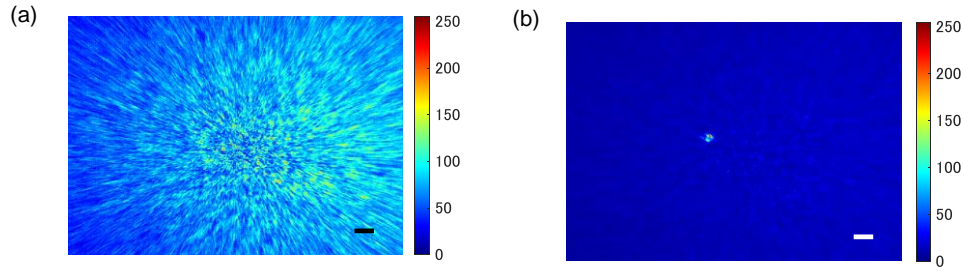


Fig. 3. (a) Unoptimized speckle pattern of the ultrashort pulse after passing through the paraffin film. Maximum intensity is scaled to 255. Scale bar is 100 μm . (b) Optimized spatially focused spot using the phase conjugation of the spectrally integrated TM for the entire wavelength region. Scale bar is 100 μm . Maximum intensity is scaled to 255.

region due to the spectral correlation of the scattered fields. Very interestingly, the observed spectra using the spectrally integrated TM at the limited wavelength range shows an enhancement, even outside the wavelength region where the spectral correlation of the speckle pattern is low. In the case of thick scattering media, the spectral width of the focused pulse is correlated to the spectral correlation width of the speckle pattern [19,20]. This is in sharp contrast with our results. Rather, the spectrally integrated TM at the limited wavelength range resembles the results obtained by “broadband” TM in a thin scattering medium where the spectral range of the refocusing capability is broader than the spectral correlation of the speckle patterns [27]. Below, we explain the origin of the enhancement of spectrally-integrated TM in a broader wavelength region compared to the spectral correlation of the speckle patterns.

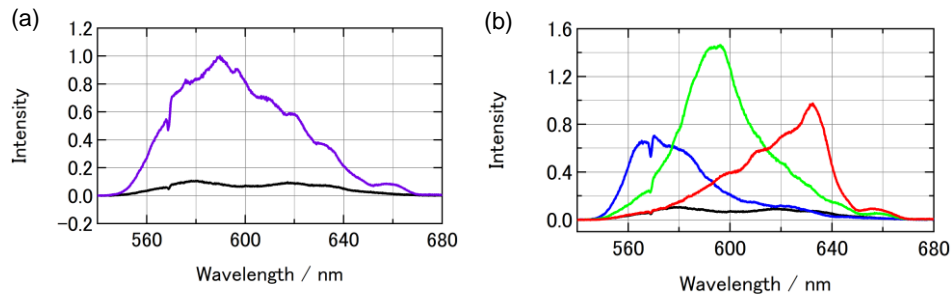


Fig. 4. (a) Spectra of ultrashort pulses transmitted through the pinhole. The black line is the unoptimized spectrum. The purple line corresponds to the optimized spectrum using the phase conjugation of the spectrally integrated TM for the entire wavelength region. Spectral intensity is normalized by the optimized spectrum. (b) Spectra of ultrashort pulses using the phase conjugation of the spectrally integrated TM at 550–570 nm (blue), 590–610 nm (green), and 630–650 nm (red) regions.

To understand the properties of the TM, we calculated the spectral cross correlation of the TM, as shown in Fig. 5. The correlation width of the spectrally resolved TM is around 8 nm, which is twice as broad as that of the speckle patterns. In contrast to multiple scattering media where the sample thickness is longer than the transport mean free path, in the current situation, the spectral range of intensity enhancement is expected to be larger than the spectral width of the speckle correlations because of the large spectral correlation of the TM. As we expect, the spectrally integrated TM has very broad correlation with the TM at each wavelength because of the in-phase

nature of each spectral component, as shown in Fig. 5(b). Figure 5(c) displays the results of the cross correlation of the spectrally integrated TM in the predefined region. The spectral correlation is similar to the band shape of focused pulses using the spectrally integrated TM in the predefined region. Even though the scattering process and dispersion effect of transparent materials distort the temporal profiles of the ultrashort pulses, the broadened pulse is still on the order of 100 fs. Therefore, interference takes place in the limited time range because the coherence of the pulse exists on a very short time scale [27]. In the common path geometry, both the pulse widths of the phase modulation and the internal reference parts are similar. When the internal reference light preserves the ultrashort-pulse nature to some extent even under the strong scattering condition, it acts as an intrinsic time-gated pulse to detect the third and fourth terms of Eq. (1). That is why the cross-correlation of the spectrally-resolved TM has broader width compared to the spectral correlation of the speckle pattern.

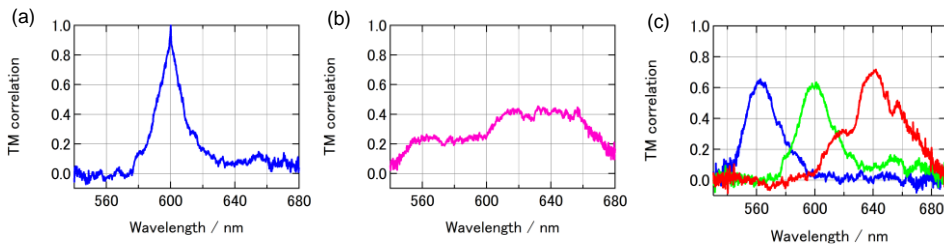


Fig. 5. (a) Cross-correlation function of spectrally resolved TMs. Correlation was calculated between spectrally-resolved TM at 600 nm and at each different wavelength. (b) Cross-correlation function between spectrally-resolved TM at each different wavelength and spectrally-integrated TM for the entire wavelength range. (c) Cross-correlation function between spectrally-resolved TM at each different wavelength and the spectrally-integrated TM at a predefined region. Blue, green, and red lines correspond to 550–570, 590–610, and 630–650 nm, respectively.

2.3. Characterization and optimization of the temporal profile of an ultrashort pulse focused at the target position

In contrast to multispectral TM measurements with an external reference pulse, the current reference pulse is not a transform-limited pulse, which means that the phase is not constant with respect to wavelength. Therefore, we have to measure the wavelength dependence of the phase of the transmitted pulses through the paraffin film to characterize their temporal profiles. To do this, we use spectral interferometry with an external reference pulse whose properties have already been characterized by MIIPS measurements [23,24]. Measurement of very weak ultrashort laser pulses were demonstrated by combining spectral interferometry and FROG. This is called TADPOLE (temporal analysis by dispersing a pair of light E-fields) [28]. From the spectral interferometry measurement, we can obtain information on the relative phase between unknown and reference pulses within a short period of time.

Figure 6 displays spectra and phase profile results of the transmitted pulses before and after optimization of wavefront shaping in the spatial domain. The wavelength dependence of the phase has a nearly parabolic structure with small bumps that corresponds to the contribution of group velocity dispersion from the glass substrate and liquid crystal layer in the SLM and paraffin films, which leads to broadening and significant distortion of the output pulses in the time domain. When we calculate the phase profile of the output pulse in the time domain passing through the thin scattering media, we added the residual phase profile of the input pulse measured by MIIPS. Furthermore, the phase profile of the output field has small wiggles and bumps that

induce complex temporal profiles in the output pulses. We can consider that the group velocity dispersion and a few scattering events inside the thin film are the main factors for determining the temporal width of the output field because the thickness of the medium (paraffin film) is longer than the scattering mean free path but shorter than the transport mean free path. Similar to the results before wavefront shaping, the wavelength dependence of the phase has a parabolic shape, which leads to the broadening and significant distortion of the output pulses in time domain. This means that TM measurement with the internal reference pulse does not allow us to optimize the temporal width of the ultrashort pulses.

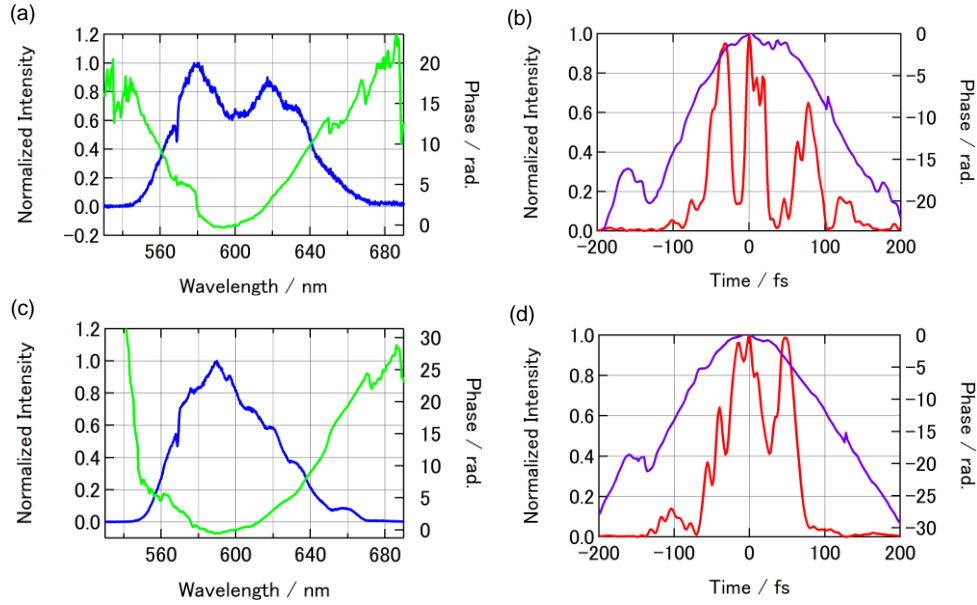


Fig. 6. (a) Spectrum (blue) and phase profile (green) of an ultrashort pulse before optimization. Phase profile is measured by spectral interferometry. (b) Temporal (red) and phase (purple) profiles of the unoptimized ultrashort pulse. (c) Optimized spectrum (blue) and phase profile (green) of an ultrashort pulse using the phase-conjugated TM for the entire wavelength region. (d) Temporal (red) and phase (purple) profiles of the optimized ultrashort pulse.

Once we know the phase profile of the output field with respect to the external reference pulse, we can compensate it by flipping the sign and encoding it in the pulse shaper, as shown in the [Supplement 1](#). It should be noted that it is not necessary to know the phase profile of the internal reference for pulse compression. To check the accuracy on the applied phase profile, we use MIIPS to retrieve the inverted phase and compare it with the phase difference between the output and external reference fields [24]. In the phase retrieval of the MIIPS technique, one has to assume that the phase profile is a continuous function with respect to the frequency. In our case, multiple pulses were observed due to scattering inside the medium. This means that phase profile has a sharp change with respect to the frequency and it is not easy to obtain fast convergence of phase retrieval. Therefore, we first fit the phase profile to a polynomial function and applied it to the pulse shaper, as shown in the [Supplement 1](#). We set the order of a polynomial function to 20. Keep in mind that the order number does not have any physical meaning. We simply express the experimentally obtained phase profile by smooth and continuous function with small deviations. Figure 7 displays the results of the retrieval of the applied phase.

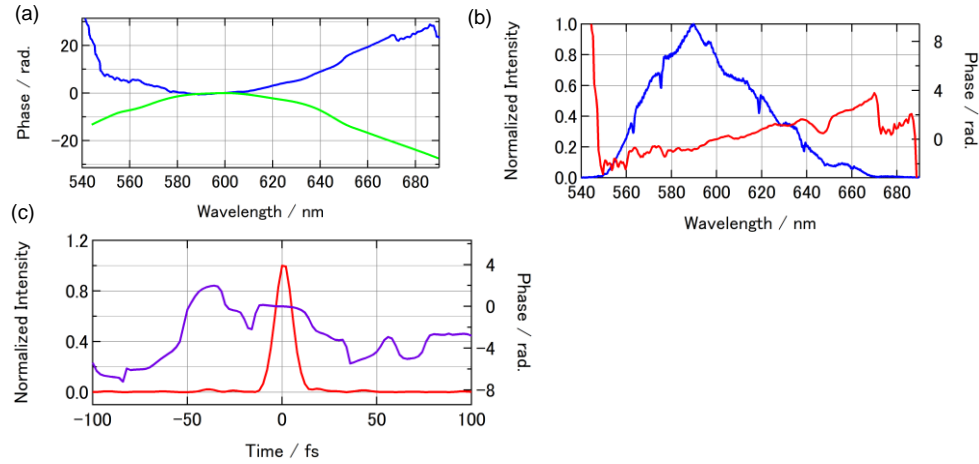


Fig. 7. (a) Phase profile of the ultrashort pulse using the phase-conjugated TM at the entire wavelength region (blue line, same as that in Fig. 6). The green line corresponds to the inverted pulse retrieved using the MIIPS measurement. (b) Spectrum of the ultrashort pulse using the phase-conjugated TM at the entire wavelength region (blue line). A smoothed function of the inverted phase profile is applied to the pulse shaper. The red line is the phase profile difference between the two data shown in (a). (c) Temporal (red) and phase (purple) profiles of the ultrashort pulse using the phase-conjugated TM. A delay time of 7 fs was added to shift the peak position to zero.

If the phase retrieval is accurate, one expects the inverted phase obtained by spectral interferometry to be equal to that applied to the pulse shaper. As shown in Fig. 7(b), the calculated phase profile has a rather linear slope. This leads to the uncertainty of the time delay, i.e., a delay time of 7 fs. As discussed in the Supplement 1, the linear term of the phase component corresponds to the time delay of the ultrashort pulse, which does not affect the second harmonic generation spectra in MIIPS measurements. Furthermore, we have some uncertainty in the value of delay time, T , in spectral interferometry. Therefore, we simply shifted the peak position of the pulse to time zero. By applying the inverted phase profile, we measured the spectrum and calculated the temporal profile of the focused output field from the results of MIIPS measurement phase retrieval. The pulse width of the focused spot is around 14 fs, which is similar to the external reference field. In this case, we added a delay time of 7 fs to shift the peak position to zero. Because of the residual small and sharp change in the phase profile, we observed small bumps in the temporal profile of the focused pulse. The intensity of the satellite structure depends on the phase structure of the focused output pulse. However, this intensity becomes much smaller than that without applying the inverted phase profile because we can compensate most of the contribution of the group velocity dispersion of the transmission optics as well as the scattering process from the paraffin film.

3. Discussion

In previous studies using a multispectral TM in thick scattering medium, temporal broadening of ultrashort pulses is characterized by the residing time of the pulse, δt , inside the scattering media [19,25]. By Fourier transforming to the frequency domain, we can define the spectral correlation width of the pulse, $\delta\omega$, which is given by the inverse of δt . Since δt is longer than the temporal width of the ultrashort pulses due to multiple scatterings inside the medium, $\delta\omega$ becomes narrower than the bandwidth of the pulses. The scattering process depends on the

wavelength of light such that different spectral components of the incident light produce different speckle patterns. This is why one can use the spectral dependence of the speckle pattern to optimize the temporal characteristics of the ultrashort pulses using wavefront shaping only in the spatial domain [19,20].

The number of independent degrees of freedom in the spectral components is given by $N = \Delta\omega/\delta\omega$, where $\Delta\omega$ corresponds to the spectral width of the ultrashort pulse [19,25]. In this case, one assumes implicitly that the temporal profile of the pulse is bandwidth-limited, i.e., Fourier transform-limited, and that the spectral phase is flat within the spectral correlation width. This means that the phase profile is a discrete quantity. One can control the spectral phase of ultrashort pulses propagating through the scattering media wherein the number of controllable spectral phases is equal to N . This assumption works well under the situation that multiple scatterings take place inside the thick scattering medium and the transport mean free path is longer than the medium thickness. In the other words, the properties of the scattering medium itself limits the number of independent phase components in the frequency domain. When N is small, this approximation does not express the quasi-continuous phase variation of the ultrashort pulses well. In the paraffin film, N is about twelve in the current setup from the measurement of the spectral correlation of the speckle patterns, as described in the [Supplement 1](#). More importantly, in the current situation, the correlation width of the spectrally resolved TM determines the number of spectral phase components, rather than the spectral correlation of the speckle patterns. Therefore, it is difficult to compensate the phase profile of the current broad spectrum only based on the multispectral TM in the spatial region because the scattering properties in the thin medium are very different from those in a thick medium. In the thin scattering media, the number of the independent phase components in the spectral domain becomes smaller compared to the thick scattering media as described before.

One may think that we can do exactly the same thing with time-gated detection of the TM, using transform-limited pulses as an external reference field [15–18]. However, to fully control the temporal profile of ultrashort pulses, a set of time-gated TM measurements are necessary at different time delays [15–18]. In this case, the number of time-gated TMs at different time delays limit the resolution of the temporal control of focused ultrashort pulses transmitted through a scattering medium. On the other hand, once we quantify the spectrally resolved TM of the scattering medium using the current method, we can manipulate the amplitude and phase profile of the output field by independently changing amplitude and phase modulations of the pulse shaper in the time domain. For example, by using the spectrally integrated TM at the wavelength range from 590 to 610 nm, we can focus ultrashort pulses at the target position. By quantifying the phase profile of this focus pulse, we can compress the pulse width to 16 fs, as shown in the [Supplement 1](#).

There are still a couple of issues that need to be improved for future application of our method. In the current setup, we can focus ultrashort pulses at a specific target spot, which is determined by the position of the pinhole. For thin scattering media, we expect to have a large angular memory effect. We consider that this will help scan the focus spot within a certain spatial range by applying a linear phase ramp in the SLM. To focus ultrashort pulses at an arbitrary position or multiple spots, TM measurements using a hyperspectral imaging technique are necessary to characterize both the spatial and spectrally resolved TM, as demonstrated by Boniface *et al.* [20]. The other drawback of the current method is that the reference field also propagates the scattering medium, which results in an inhomogeneous distribution of the amplitude of the reference field. Very recently, Hofer and Brasselet proposed a method to compensate inhomogeneous distribution of the internal reference field from a thin scattering medium using the angular memory effect [29]. By using this method, one can achieve a uniform sensitivity of the TM in terms of the target positions.

Finally, we briefly comment on the spatiotemporal control of a tunable continuous-wave light propagating in disordered media such as multimode fiber with the external reference light [30–32]. We can perform similar approach by using pulse shaper in time domain as a tunable narrowband filter in frequency domain. Different from a swept laser source, the intensity of narrowband pulse becomes lower and more averaging of the signal is necessary when one wants to obtain the same quality of the data. Even though the measurement time of the spectrally-resolved TM is going to be long, we will be able to characterize the TM in multiple positions simultaneously by a camera without using the spectrometer. Paudel *et al.* demonstrated to focus the broadband superluminescent diode light through the scattering media by optimizing the spectrally integrated intensity with the nonlinearity parameter. They found that sub-linear value of the nonlinearity parameter leads to the increase of the spectral bandwidth. We can apply it to control the spectral bandwidth of the ultrashort pulses focused at the target position [33]. McCabe *et al.* demonstrated that the temporal profile of the output speckle passing through a thick scattering medium can be recompressed using a pulse shaper in the time domain. In that method, one cannot expect the enhancement of the linear intensity at the target position because one can change only the temporal profile of the ultrashort pulse, not the time-integrated intensity [34,35]. Recently, Buchau *et al.* demonstrated the correction of the wavefront distortion and enhancement of the fluorescence signals in a two-photon microscope with spatial and temporal pulse shapers [36]. However, the sample was a dye solution with a cover glass so that only small correction of the wavefront is necessary to optimize the signals. They used the SLM simply as an adaptive optics which is totally different from the wavefront shaping in the current study.

One may think the application of the current method to thick scattering media. By using spectrally integrated TM or broadband TM methods, we can focus ultrashort pulses to the target position. Owing to the copropagating geometry of the TM measurement with the internal reference pulse, the temporal profile of the pulse becomes longer and has multiple peaks because of interference of the pulses with different time delays [25]. By using the pulse shaper in the time domain, we can compensate the complex phase profile to compress the temporal width of the pulse. One of the major differences between thin and thick scattering media is that we expect to observe a complex interference pattern in the spectrum in the frequency domain when an ultrashort pulse passes through thick scattering media [25]. This means that the compressed ultrashort pulse has many satellite peaks in the time domain when we only apply phase modulation to the pulse shaper [34]. When we use both amplitude and phase modulation in the pulse shaper, we can manipulate the amplitude profile to obtain a smoother spectral shape. This will help decrease the intensity of the satellite peaks. This is different from the situation when one only uses the multispectral TM method to focus ultrashort pulses at the target position and to optimize the temporal profile of such pulses [19].

In summary, we have demonstrated that spectrally resolved TM with an internal speckled reference and the spectral interferometry with the external reference can be applied to focus ultrashort pulses at the target position through a thin scattering medium. Even if the phase profile of the internal reference field is unknown, we can characterize the phase profile of the focused field using spectral interferometry with the external reference pulse. We have found that a positive chirp in transmission-type optics and a small number of scattering events in thin films lead to significant distortion of the temporal profile of ultrashort pulses. By combining the spectrally integrated TM measurement with a pulse shaper in the time domain, we can optimize the temporal width of the output field by flipping the sign of the obtained phase profile and focus the ultrashort pulses at the target position in a time-reversed manner. This will open the possibility to use ultrashort 10-fs pulses in a variety of spectroscopic methods, even in strongly scattering conditions. In particular, any signals based on nonlinear optical process are sensitive to the pulse width such that optimization of the amplitude and phase profile of the ultrashort

pulses drastically changes the quality of the signals and image contrast on a very fast time scale in nonlinear optical spectroscopy and microscopy [6–8].

Funding. Japan Society for the Promotion of Science (16K13934, 21H05594, 24655017); Japan Science and Technology Agency (PRESTO program).

Acknowledgements. We thank Professor Keisuke Tominaga, Dr. Nobuyuki Nakagiri, and Professor Hiroshi Masuhara for invaluable discussions and continuous encouragement. We also thank the administrator of the website “<http://wavefrontshaping.net>” for providing a lot of insightful information.

Disclosures. The author declares no conflicts of interest.

Data Availability. Data may be obtained from the authors upon reasonable request.

Supplemental document. See [Supplement 1](#) for supporting content.

References

1. A. Stingl, M. Lenzner, C. Spielmann, F. Krausz, and R. Szipocs, “Sub-10-fs mirror-dispersion-controlled Ti:sapphire laser,” *Opt. Lett.* **20**(6), 602–604 (1995).
2. A. Shirakawa, I. Sakane, and T. Kobayashi, “Pulse-front-matched optical parametric amplification for sub-10-fs pulse generation tunable in the visible and near infrared,” *Opt. Lett.* **23**(16), 1292–1294 (1998).
3. G. Cerullo, M. Nisoli, S. Stagira, and S. De Silvestri, “Sub-8-fs pulses from an ultrabroadband optical parametric amplifier in the visible,” *Opt. Lett.* **23**(16), 1283–1285 (1998).
4. A. M. Weiner, “Femtosecond pulse shaping using spatial light modulators,” *Rev. Sci. Instrum.* **71**(5), 1929–1960 (2000).
5. A. Monmayrant, S. Weber, and B. Chatel, “A newcomer’s guide to ultrashort pulse shaping and characterization,” *J. Phys. B: At., Mol. Opt. Phys.* **43**(10), 103001 (2010).
6. M. Liebel, C. Toninelli, and N. F. van Hulst, “Room-temperature ultrafast nonlinear spectroscopy of a single molecule,” *Nat. Photonics* **12**(1), 45–49 (2018).
7. A. C. Jones, N. M. Kearns, J.-J. Ho, J. T. Flach, and M. T. Zanni, “Impact of non-equilibrium molecular packings on singlet fission in microcrystals observed using 2D white-light microscopy,” *Nat. Chem.* **12**(1), 40–47 (2020).
8. J. Sung, C. Schnedermann, L. Ni, A. Sadhanala, R. Y. S. Chen, C. Cho, L. Priest, J. M. Lim, H.-K. Kim, B. Monserrat, P. Kukura, and A. Rao, “Long-range ballistic propagation of carriers in methylammonium lead iodide perovskite thin films,” *Nat. Phys.* **16**(2), 171–176 (2020).
9. J. Aulbach, A. Bretagne, M. Fink, M. Tanter, and A. Tourin, “Optimal spatiotemporal focusing through complex scattering media,” *Phys. Rev. E* **85**(1), 016605 (2012).
10. I. M. Vellekoop and A. P. Mosk, “Focusing coherent light through opaque strongly scattering media,” *Opt. Lett.* **32**(16), 2309–2311 (2007).
11. S. M. Popoff, G. Lerosey, R. Carminati, M. Fink, A. Boccarda, and S. Gigan, “Measuring the transmission matrix in optics: an approach to the study and control of light propagation in disordered media,” *Phys. Rev. Lett.* **104**(10), 100601 (2010).
12. M. Cui and C. H. Yang, “Implementation of a digital optical phase conjugation system and its application to study the robustness of turbidity suppression by phase conjugation,” *Opt. Express* **18**(4), 3444–3455 (2010).
13. S. Rotter and S. Gigan, “Light fields in complex media: Mesoscopic scattering meets wave control,” *Rev. Mod. Phys.* **89**(1), 015005 (2017).
14. O. Katz, E. Small, Y. Bromberg, and Y. Silberberg, “Focusing and compression of ultrashort pulses through scattering media,” *Nat. Photonics* **5**(6), 372–377 (2011).
15. J. Aulbach, B. Gjonaj, P. M. Johnson, A. P. Mosk, and A. Lagendijk, “Control of light transmission through opaque scattering media in space and time,” *Phys. Rev. Lett.* **106**(10), 103901 (2011).
16. A. P. Mosk, A. Lagendijk, G. Lerosey, and M. Fink, “Controlling waves in space and time for imaging and focusing in complex media,” *Nat. Photonics* **6**(5), 283–292 (2012).
17. Y. Choi, T. R. Hillman, W. Choi, N. Lue, R. R. Dasari, P. T. C. So, W. Choi, and Z. Yaqoob, “Measurement of the time-resolved reflection matrix for enhancing light energy delivery into a scattering medium,” *Phys. Rev. Lett.* **111**(24), 243901 (2013).
18. M. Mounaix, H. Defienne, and S. Gigan, “Deterministic light focusing in space and time through multiple scattering media with a time-resolved transmission matrix approach,” *Phys. Rev. A* **94**(4), 041802 (2016).
19. M. Mounaix, D. Andreoli, H. Defienne, G. Volpe, O. Katz, S. Gresillon, and S. Gigan, “Spatiotemporal coherent control of light through a multiple scattering medium with the multispectral transmission matrix,” *Phys. Rev. Lett.* **116**(25), 253901 (2016).
20. A. Boniface, I. Gusachenko, K. Dholakia, and S. Gigan, “Rapid broadband characterization of scattering medium using hyperspectral imaging,” *Optica* **6**(3), 274–279 (2019).
21. D. Andreoli, G. Volpe, S. Popoff, O. Katz, O. S. Gresillon, and S. Gigan, “Deterministic control of broadband light through a multiply scattering medium via the multispectral transmission matrix,” *Sci. Rep.* **5**(1), 10347 (2015).
22. L. Lepetit, G. Cheriaux, and M. Joffe, “Linear techniques of phase measurement by femtosecond spectral interferometry for applications in spectroscopy,” *J. Opt. Soc. Am. B* **12**(12), 2467–2474 (1995).

23. V. V. Lozovoy, I. Pastirk, and M. Dantus, "Multiphoton intrapulse interference. IV. Ultrashort laser pulse spectral phase characterization and compensation," *Opt. Lett.* **29**(7), 775–777 (2004).
24. B. Xu, J. M. Gunn, J. M. Dela Cruz, V. V. Lozovoy, and M. Dantus, "Quantitative investigation of the multiphoton intrapulse interference phase scan method for simultaneous phase measurement and compensation of femtosecond laser pulses," *J. Opt. Soc. Am. B* **23**(4), 750–759 (2006).
25. M. Mounaix, H. B. de Aguiar, and S. Gigan, "Temporal recompression through a scattering medium via a broadband transmission matrix," *Optica* **4**(10), 1289–1292 (2017).
26. E. Small, O. Katz, and Y. Silberberg, "Spatiotemporal focusing through a thin scattering layer," *Opt. Express* **20**(5), 5189–5195 (2012).
27. A. G. Vesga, M. Hofer, N. K. Balla, H. B. de Aguiar, M. Guillon, and S. Brasselet, "Focusing large spectral bandwidths through scattering media," *Opt. Express* **27**(20), 28384–28394 (2019).
28. D. N. Fittinghoff, J. L. Bowie, J. N. Sweetser, R. T. Jennings, M. A. Krumbugel, K. W. DeLong, R. Trebino, and I. A. Walmsley, "Measurement of the intensity and phase of ultraweak, ultrashort laser pulses," *Opt. Lett.* **21**(12), 884–886 (1996).
29. M. Hofer and S. Brasselet, "Manipulating the transmission matrix of scattering media for nonlinear imaging beyond the memory effect," *Opt. Lett.* **44**(9), 2137–2140 (2019).
30. W. Xiong, C. W. Hsu, and H. Cao, "Long-range spatio-temporal correlations in multimode fibers for pulse delivery," *Nat. Commun.* **10**(1), 2973 (2019).
31. M. Mounaix and J. Carpenter, "Control of the temporal and polarization response of a multimode fiber," *Nat. Commun.* **10**(1), 5085 (2019).
32. M. Mounaix, N. K. Fontaine, D. T. Neilson, R. Ryf, H. Chen, J. C. Alvarado-Zacarias, and J. Carpenter, "Time reversed optical waves by arbitrary vector spatiotemporal field generation," *Nat. Commun.* **11**(1), 5813 (2020).
33. H. P. Paudel, C. Stockbridge, J. Mertz, and T. Bifano, "Focusing polychromatic light through strongly scattering media," *Opt. Express* **21**(14), 17299–17308 (2013).
34. D. J. McCabe, A. Tajalli, D. R. Austin, P. Bondareff, I. A. Walmsley, S. Gigan, and B. Chatel, "Spatio-temporal focusing of an ultrafast pulse through a multiply scattering medium," *Nat. Commun.* **2**(1), 447 (2011).
35. M. C. Velsink, L. V. Amitonova, and P. W. H. Pinkse, "Spatiotemporal focusing through a multimode fiber via time-domain wavefront shaping," *Opt. Express* **29**(1), 272–290 (2021).
36. F. Buchau, A. Patas, Y. Yang, A. Lindinger, and K. Heyne, "A stage-scanning two-photon microscope with a temporal and spatial pulse shaper: Enhance fluorescence signal by phase shaping," *Rev. Sci. Instrum.* **89**(12), 123701 (2018).